Macromolecules 1994, *27*, 6443-6451

Determination of an Interpenetrating Network Structure by Small-Angle Neutron Scattering

Jyotsana Lal,[†] Jean Michel Widmaier,[‡] Jacques Bastide,[‡] and Francois Boué*[,§]

Collège de France, Physique de la Matière Condensée, 11 Place Marcelin Berthelot, 75231 Paris Cedex 05, France, Institut Charles Sadron, (CRM-EAHP), CNRS-ULP, 6 rue Boussingault, 67083 Strasbourg Cedex, France, and Laboratoire Léon Brillouin, (CEA-CNRS), CEN, Saclay, 91191 Gif-Sur-Yvette Cedex, France

Received December 28, 1993; Revised Manuscript Received June 9, 1994[®]

ABSTRACT: Small-angle neutron scattering (SANS) was used to study the effects of cross-link density on the structure of in situ sequential interpenetrating polymer networks (IPNs). The system investigated is a PSD (deuterated polystyrene-*co*-divinylbenzene) network built within a matrix network of PUR (polyurethane). The scattering can be approximated by the Debye–Bueche law with a q^{-4} dependence at intermediate values of wave vector q, with departures from it at both low and very large values of q. At low q, this Debye–Bueche law yields a value of the structure factor $S(q \rightarrow 0)$ and a correlation length ξ. At large q, it yields a value of the specific area S/V S being the total area and V the total volume. As the cross-link density of either network of the IPN increases, $S(q \rightarrow 0)$ and ξ decreases, while S/V increases. The measured ξ is in the range 20 to 80 Å and the values of S/V correspond to 100–300 m^2/gm, indicating a rather finely divided material. The quantity $S(q \rightarrow 0)$, after being divided by volume ξ^3, allows us to estimate the contrast. The existence of a maximum in $S(q)$ is discussed for the most cross-linked samples. With increasing cross-link density of the networks, it seems that the size of phase-separated regions is decreasing, indicating that the IPN structure freezes earlier in the evolution of the separation kinetics. However, from comparison of effective contrast and maximum contrast between "pure phases" (i.e. made of pure PSD and the other of pure PUR), it seems that the content of the separated regions is closer to "pure phases" when the cross-linking is higher. At this stage of the analysis, the effects of complicated topological connectivity between the two networks were neglected.

I. Introduction

Generally two dissimilar polymers will be thermodynamically immiscible with one another, making a simple mixture of such polymers segregate completely. The mode of association of polymers in the form of their interpenetrating networks (IPNs) is known to reduce their degree of phase separation.[1] As the miscibility of such networks increases, the glass transition behavior changes from two distinct transitions, i.e. one for each polymer network, toward one broad transition in a systematic manner. A deeper understanding of their structure and behavior could lead to synthesis of novel materials with desired properties.

There are two submethods of synthesis of IPNs: the first one produces in situ simultaneous IPNs in which oligomers and monomers of chain types A and B are mixed together with their specific cross-linking agents and initiators and the resulting mixture is cured to produce the networks.[2] The second one produces in situ sequential IPNs in which a cross-linked network is first obtained and then is swollen by the monomer of the other species, its cross-linking agent and its initiator, or catalyst, thus the second network is formed inside the first one.[3] In general two very different IPNs result depending on their mode of synthesis. There also exist pseudo-IPNs or semi-IPNs which consists of network of one polymer A(B) swollen by linear un-cross-linked polymer chains of A(B).[4]

IPNs have been extensively studied in the past. The kinetics of formation of polyurethane/polymethylmethacrylate networks[5] (i.e. *net*-poly(urethane)-*internet*-poly(methylmethacrylate) in the IUPAC nomenclature) has been studied by Fourier transform infrared (FTIR) spectroscopy[5] and the glass transitions by dynamic mechanical measurements.[2] The study of the glass transition temperatures does not give a direct measurement of the extent of demixing in such systems. Turbidity measurements by light scattering give the extent of heterogeneities as a function of cross-link density and internetwork grafting in polyurethane/polystyrene IPNs[3]. Small-angle neutron scattering (SANS) techniques may also yield precise and useful investigation of structure of such networks by using deuteration for better contrast. It can (i) reveal heterogeneities on length scales of a few angstroms to several hundred angstroms, (ii) give information about the type of interface being formed between the demixed regions, e.g. whether it is diffuse or sharp, and (iii) give the total interfacial area. SANS experiments have already been performed on poly(dimethylsiloxane)/polystyrene[6] IPNs and poly(dimethylsiloxane)/polymethacrylic acid[7] IPNs. Also, for poly(butadiene)/polystyrene[8] IPNs, the interfacial area was estimated from SANS experiments. Networks containing a certain fraction of deuterated primary chains made possible the determination of the radius of gyration as the polymerization proceeded.[9] Poly(carbonate urethane) (PCU)/poly(vinylpyrridine) IPNs which are simultaneously formed display a maximum in the scattering for large content of PCU, i.e. for the case of the most cross-linked of the two networks.[10]

We investigate here an in situ sequential IPN made from poly(oxypropylene glycol)-based polyurethane and deuterated polystyrene-*co*-divinylbenzene (PUR/PSD).[3] It is generally believed that the network formed first governs, to some extent, the formation of the second network.[5,11] Following this picture, the PUR network in the present IPNs may be regarded as the matrix and the PSD as the dispersed phase, representing the heterogeneities of the material. It was already shown[3] that variation

---

[†] Collège de France.
[‡] Institut Charles Sadron.
[§] Laboratoire Léon Brillouin.
[®] Abstract published in *Advance ACS Abstracts*, July 15, 1994.

0024-9297/94/2227-6443$04.50/0

of the cross-link density of the PUR network plays a more important role than that of PSD, which shows the importance of the tridimensional structure formed first in an IPN.

A simple picture of such system is that as soon as the monomers polymerize into chains of large molecular weight (reducing their translational entropy) or into branched polymers, they tend to phase separate (this stage is similar for both simultaneous and sequential IPNs). On further cross-linking, the phase-separated regions connect and form a bicontinuous system of interpenetrated phases. Further demixing is limited, maybe not just on a molecular level by the cross-linking, but by an average elasticity of each of the connecting networks, i.e. on a scale larger than the mesh size.

One can consider some more sophisticated mechanisms of demixing: the first one is spinodal decomposition where a periodic structure develops with a characteristic cutoff length, associated with a maximum in the structure factor frozen by the cross-linking or the continuous medium elasticity.[12]

The second mechanism is related to the spatial distribution of free chains in a network. Here, free chains would be the transient free chains before they form a fully connecting network. There are two contradictory regimes. In the first one, the network expels the chains (in order to reduce the elastic energy it costs which is not balanced by their low translational entropy, when the network is swollen by the guest chains). In the second regime, the network limits the clustering of the free chains. The first regime was seen in practice for networks[13,14] and gels.[4] In both cases the scattering is much weaker than for a fully phase-separated system. It was proposed that the free chains invade the soft regions of the network and thus reveal the heterogeneities of the network; this is equivalent to weak segregation and $S(q) \approx q^{-2.5}$. In a similar way the heterogeneities of the first network could be revealed by the second network growing in the soft regions. In ref 4, by removing the solvent (which keeps the free chains and the network chains partially compatible), we strongly increase the Flory interaction parameter leading to strong segregation of $S(q) \approx q^{-4}$ instead of the weak one of $S(q) \approx q^{-2.5}$ observed before.

The limiting effect of the structure can be at the size of the mesh if the network is very regular. It was proposed by deGennes[15] that a grafted IPN made of strands of A polymer co-cross-linked with strands of B polymer would exhibit a microphase separation similar to the case of block copolymers. It is likely that similar effects would occur for more or less regular networks (probably strongly cross-linked) if the interpenetration is made prior to separation, as proposed in order to explain the results of PVME/PSD IPN's[16] where the phase separation is provoked after cross-linking by increasing the temperature. (PVME/PSD mixtures exhibit a LCST phase diagram; a shoulder or a maximum was observed in the scattering of cross-linked samples.)

II. Experimental Section

Synthesis of IPNs. The synthesis is defined as "in situ sequential". This means that the starting mixture already contains all the chemicals necessary for the building of the two networks. The first network is synthesized at room temperature and consequently, the second one is built afterward by raising the temperature.

The first network is formed from poly(oxypropylene glycol) (POPG, ARCO Chemical) chains. The analysis of the OH groups show that POPG has a functionality of approximately 2. Their extremities are OH groups, which react with the NCO groups of an aliphatic pluriisocyanate, mainly trifunctional, (Desmodur N, Bayer AG). In presence of stannous octoate (Goldschmidt) as catalyst, this condensation reaction leads to urethane bonding, thus the first-formed network is polyurethane (PUR).

Table 1. Composition of the PUR/PSD IPNs

	PUR		PSD	
sample	% PUR total	M_n of PUR chain	% PSD total	DVB content
W1	100	2000	0	0
W2	0		100	3/103
W3	34	2000	66	3/103
W6	34	3025	66	3/103
W7	34	450	66	3/103
W4	34	2000	66	0/100
W5	34	2000	66	12/112

The second network is made by free-radical copolymerization of styrene (deuterated-S-d_8, Aldrich) with divinylbenzene (DVB, Merck). As DVB molecules copolymerize between themselves as well as with styrene, the junctions can be cluster like, with a large functionality. 2,2′-azobisisobutyronitrile (AIBN, Merck), which decomposes at 60 °C, was used as free-radical initiator.

The weight fraction of the PUR network is 34% (POPG and Desmodur N), hence for the PSD network it is 66%. The contents, in the starting mixture for each sample, of POPG, Desmodur, styrene, and DVB are listed in Table 1. The cross-link density of the PUR network have been varied by using three different molecular weights of POPG chains. The average molecular weights M_n between cross-links given in Table 1 correspond to the molecular weight of the polyol (POPG). The cross-link density of the PSD network was varied by changing the amount of DVB.

Gelation of the PUR network occurred at room temperature within 30 min, using 1% catalyst by weight. Then, the temperature was raised to 60 °C for the PSD network synthesis, after complete reaction (at least 2 h at room temperature). After 15 h, the samples were removed from the mold and annealed under vacuum at 120 °C for at least 2 h.

SANS. The neutron scattering experiments were carried out on a small-angle neutron spectrometer, PACE, at the Laboratoire Léon Brillouin, Saclay. The data were taken at four different configurations:

	sample-detector distance: D (m)	wavelength: λ (Å)	q (Å^{-1})
(1)	3.50	14.86	$0.0036 < q < 0.0384$
(2)	3.00	12.20	$0.0051 < q < 0.0540$
(3)	2.50	7.98	$0.0095 < q < 0.1000$
(4)	1.20	5.50	$0.0280 < q < 0.290$

The scattering was performed at room temperature. The data were collected by annular cells of the detector. Superimposed with the above data is another set from ILL in the q range $0.0025 < q < 0.0118$ Å^{-1}.

The raw data were treated for scattering from empty cell, sample thickness, transmission, detector efficiency, and normalization to units cm^{-1} (by dividing by a water spectrum). The last treatment required is a careful subtraction of the incoherent background, due to the hydrogen and deuterium nuclei. At this point the interest is in coherent scattering from structure due to the mixture of the two components. Under the simplest assumption all the "coherent signal" comes from this structure, and then one has to subtract the normalized incoherent signal of the PUR and PSD networks alone. In principle, the measured scattering $S_{PUR}(q)$ and $S_{PSD}(q)$ of the samples W1 (pure PUR network) and W2 (pure PSD network) should be "incoherent", and thus equal to constants, B_{PSD} and B_{PUR}, with no q dependence. In these conditions, one would subtract the following contribution of the incoherent scattering:

$$S_{\text{incoherent}} = \phi_{PSD} B_{PSD} + (1 - \phi_{PSD}) B_{PUR} \qquad (1)$$

Although in practice the scattering from W1(PUR) is nearly flat, the one from W2(PSD) has a q dependence, i.e. a strong increase of signal at low q. The origin of this signal is unknown.

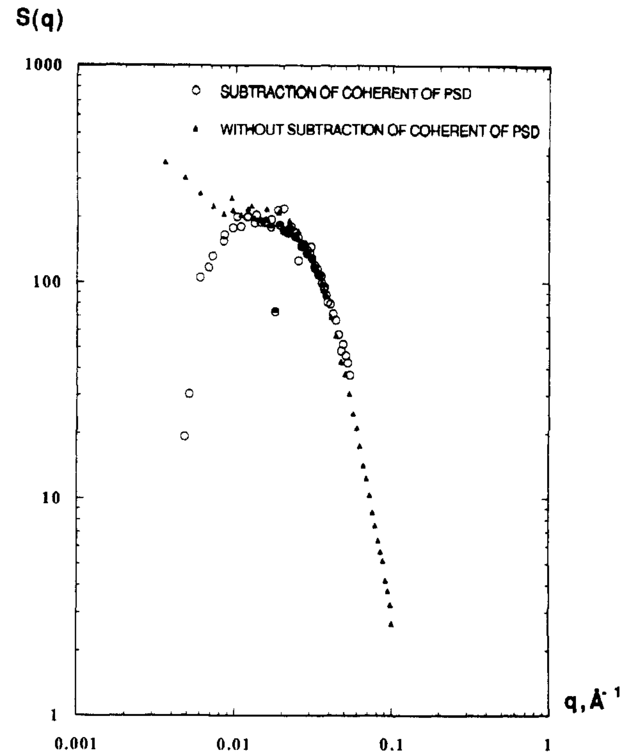

Figure 1. log $S(q)$ vs log q for $M_n = 450$ with and without subtraction of the signal of PSD at low q.

One possibility could be the clustering of DVBs; however, in case of pure PSD comparable behavior is usually observed and often attributed to voids.[17] The incoherent contribution can be taken equal to $B_{\mathrm{PSD}} = S_{\mathrm{PSD}}(q \rightarrow \infty)$.

There are two options: (i) Subtract a flat incoherent background

$$S_{\mathrm{incoherent}} = \phi_{\mathrm{PSD}}S_{\mathrm{PSD}}(q \rightarrow \infty) + (1 - \phi_{\mathrm{PSD}})S_{\mathrm{PUR}} \qquad (2)$$

Such a subtraction is important at large q only ($q > 10^{-2}$ Å^{-1}). The value of $S_{\mathrm{incoherent}}$ is 0.7 cm^{-1}. (ii) Subtract a q-dependent background

$$S_{\mathrm{incoherent}}(q) = \phi_{\mathrm{PSD}}B_{\mathrm{PSD}}(q) + (1 - \phi_{\mathrm{PSD}})B_{\mathrm{PUR}} \qquad (3)$$

which is not totally flat, as there is a large contribution at $q < 10^{-2}$ Å^{-1}. Both treatments of the data were done. A difference exists for $q < 10^{-2}$ Å^{-1}. For all samples except the most cross-linked $M_n = 450$ and 10.7% DVB the difference between the two types of treatments is not very important. By using the first option a small upturn at low q is seen and it is not very clean or smooth. By using the second option the main difficulty is not knowing how $S_{\mathrm{incoherent}}(q)$ varies with cross-linking and used as such a priori it is not clear whether the right background is being subtracted for each sample. Here all data is presented using the first option. Thus, one observes at very small q, an upturn in each sample, more or less pronounced. This low q upturn will be fitted to a scattering law below, but still it is not known whether it has the origin just from the PSD alone. If one would use the second option, the upturn is reduced in most of the case. For sample $M_n = 450$, it even transforms into a decreasing behavior: i.e. one observes a *maximum* in $S(q)$. The two options are shown in Figure 1.

The scattering was normalized by water which was used as a standard and is in absolute units (cm^{-1}) using the correction of Oberthur.[18] This yields $S(q)$ which is the cross section per unit volume. The scattering as shown in Figures 2 and 3 is strong at low q, ≈1000 cm^{-1}. Here, the effects of multiple scattering could not be excluded; another indication of it may be that the data in the different q ranges are better superimposed after slight corrections. Finally, in the low the q range, where multiple scattering maybe important, the measured transmissions of the samples are low compared to the higher q range. The only way to overcome the difficulty would be to use even thinner samples

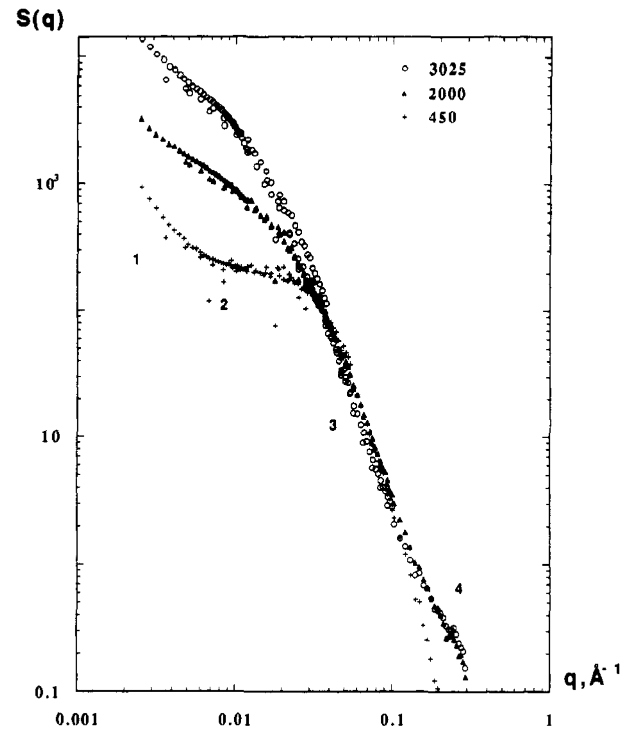

Figure 2. Plot of log $S(q)$ vs log q for various cross-link densities of PUR network keeping the density of PSD fixed at 3% DVB. The numbers 1–4 indicate the different regimes of q.

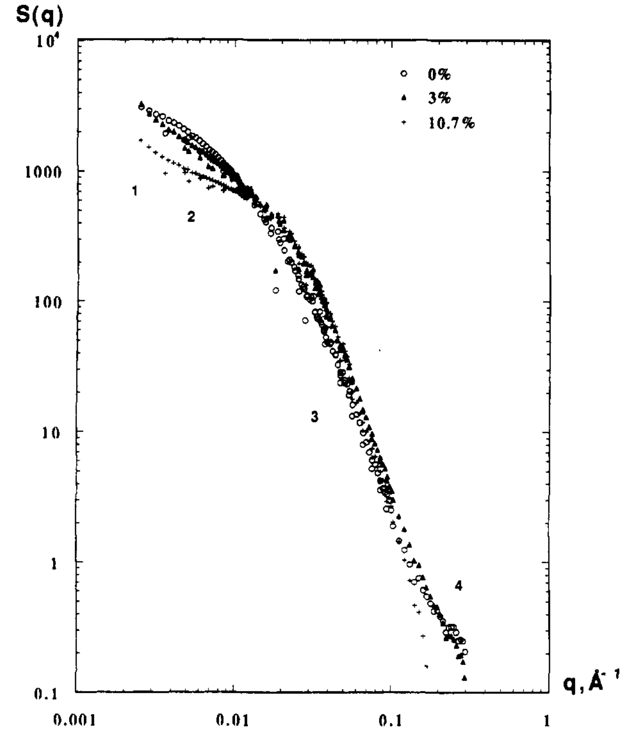

Figure 3. Plot of log $S(q)$ vs log q for various cross-link densities PSD network keeping the density of PUR fixed at $M_n = 2000$. The numbers 1–4 indicate the different regimes of q.

than the average value of 0.7 mm used here. This was done in the more recent measurements, which showed that the low q signal in absolute units, i.e. divided by the thickness and transmission was higher, when the sample was thinner. A simple explanation for the low transmission could be enhanced inelastic scattering due to multiple scattering. The cold neutrons (e.g. at 15 Å) are "heated" through the successive scattering events, which leads to a lowering of their wavelength. The apparent signal at a given angle, attributed to $q = (4\pi/\lambda)\sin(\theta/2)$, is actually corresponding to a higher q value, and thus is smaller. A good criterion for multiple scattering is that part of attenuation of the direct beam due to coherent scattering should not be <0.9. This is not met for sample W6 for which data are taken only as indicative, and will be discussed below for other samples.

III. Results

Qualitative Variations. In Figure 2, on a log $S(q)$ versus log q plot, the data are represented for three different cross-link densities of the PUR network (M_n = 450, 2000, and 3025), at constant cross-link density of DVB equal to 3% of the second network (PSD) of the IPN. Similarly in Figure 3, the data is represented for the three different cross-link densities of the PSD network (% DVB = 0%, 3%, and 10.7%), at constant cross-link density M_n = 2000 of the first network (PUR) of the IPN.

In all cases the scattering curves can be divided into four regions: At low q, region 1, the signal decreases strongly with q. In region 2, there is a relatively flat part, in other words a shoulder. In region 3, the decrease is strong with a −4 slope (q^{-4}). In region 4, one observes a deviation from this slope: either the decrease is slower for samples less cross-linked (2000 or 3025 and 0%), tending to a slope of −2, or it is steeper, for the samples more cross-linked (450 and 10.7%). Trying to modify the background subtraction, even more than is realistic, does not change the conclusions.

The upturn of scattering at the lowest q values (region 1) will vary depending on the subtraction of the background signal of the PSD sample. For samples M_n = 2000 and 3025, this variation is not large. However, for sample M_n = 450, which scatters less at low angles, the difference is significant, because as said above the upturn transforms into a downturn, leading to maximum in $S(q)$ with the subtraction of the background of PSD as shown in Figure 1. In the region 1 and 2, the signal depends strongly on cross-link density: the stronger the cross-linking, the smaller the $S(q)$. An obvious interpretation is that the phase separation is reduced by cross-linking: it will be discussed in greater detail below. At intermediate values of q (region 3), one observes a q^{-4} variation which corresponds to the well-known Porod's law. The prefactor in Porod's law is the specific area, which is lower when the scattering objects are larger: thus the curves for different cross-linking cross each other, $S(q)$ for low cross-link ratio being larger at low q and smaller at large q.

These features are also present in Figure 3, for all the samples being at the same cross-link ratio of the PUR network (M_n = 2000). However, the variation of $S(q)$ with cross-link densities of the second network (PSD) seems lower, as expected from other measurements.[6] From a comparison of Figures 2 and 3, it is obvious that varying the cross-link density of the PUR network has a more dramatic effect than that of the PSD particularly at low q. In the next section an attempt will be made toward a more quantitative basis for the above description.

Multiple Scattering. For the configurations where short wavelengths (5 Å) were used, the part T_{coh} of attenuation of the direct beam due to coherent scattering was low, i.e. with values around 0.8. T_{coh} is obtained by dividing the transmission T of the IPNs by transmission T_r ($T_{\mathrm{coh}} = T/T_r$). T_r (extracted from the incoherent background) is defined as $e^{-(\mu_{\mathrm{PSD}}\phi_{\mathrm{PSD}}+\mu_{\mathrm{PUR}}\phi_{\mathrm{PUR}})t}$ where t is the thickness of the IPN sample, $\mu_{\mathrm{PSD}} = -\log(T_{\mathrm{PSD}})/t_{\mathrm{PSD}}$, i.e. T_{PSD} is transmission of pure PSD sample at a particular configuration, ϕ_{PSD} is the fraction of PSD, and t_{PSD} is the thickness of the PSD sample (with a similar set of definitions for pure PUR sample). This may be due to the fact that the transmission measurement records both the transmitted beam and a part of the scattered beam at low angles, but also at the same time the inelastic multiple scattering is not important here. On the contrary for low q configurations involving large wavelengths (e.g. >14 Å), T_{coh} can be as low as 0.5. However, the data of all samples are creditable except W6 for two reasons: First, data of different configurations overlap within the accuracy of the analysis and can be fitted by a single function (see below). Second, a check was done using a short wavelength (5 Å) and large distance (5 m) on W3, leading to good overlapping on the range 8×10^{-3} Å^{-1} to 10^{-1} Å^{-1} with the other data shown here. Sample W6 displays a very strong scattering, a very low T_{coh}, and systematic bad overlapping between the large q's of configuration (i) and the low q of configuration (i + 1). The main effect is that the large q scattering is artificially increased,[19] which leads to a weaker variation of $I(q)$; for example it may make an apparent a cutoff of the increase of $I(q)$ (when going from large q to low q) at $q \approx 1/\xi_{\mathrm{app}} \gg 1/\xi_{\mathrm{real}}$.

Table 2. Glass Transition Temperatures (T_g's) of the PUR/PSD IPNs

	T_g	
	Pure PUR	
3025 g/mol	−61.7 °C	
2000 g/mol	−56.2 °C	
450 g/mol	−12.9 °C	
	Pure PSD	
linear (0% DVB)	97 °C	
cross linked (3% DVB)	100 °C	
cross linked (10.7% DVB)	101–103 °C	
	IPN 34/66 –PSD Cross-Linked at 3% DVB	
3025 g/mol	no data	
2000 g/mol	two *T*g's	−51.5 °C and 81.0 °C
450 g/mol	two *T*g's	5.7 °C and 74.5 °C
	IPN 34/66 –For 2000 g/mol of POPG	
0% DVB	two *T*g's	−55.3 °C and 94.5 °C
3% DVB	two *T*g's	−51.5 °C and 81.0 °C
10.7% DVB	no data	

Glass Transition Temperatures. The glass transition temperatures (T_g) were measured by differential scanning calorimetry (DSC, Perkin-Elmer) for some of the IPN samples and parent networks are given in Table 2. All samples exhibit two *T*g's. For the pure networks, *T*g's increase with cross-linking and for the IPNs the two *T*g's are shifted "inward". The effect is stronger for the most cross-linked IPN for which data are available (W7).

Quantitative Analysis of Data: Debye–Bueche Law. Volume Fractions and Maximum Contrast. Let us first focus in the scattering regions 2 and 3: for all data, when decreasing q, the q^{-4} scattering saturates or stops around a certain value $q \approx 1/\xi$. This implies that there is a cutoff length ξ in the system. For lengths below ξ ($q > 1/\xi$), one has Porod's law. A general treatment of scattering from an inhomogeneous solid[20] yields such a behavior. This law assumes a random distribution of the two phases at any scale. It was applied successfully[21] for X-ray scattering by porous material, where a random distribution of holes of different sizes and shapes can be characterized by an exponential correlation function, $\exp(-r/\xi)$, where ξ is the characteristic length in the system. For such a correlation function, the reciprocal square root of the scattered intensity is proportional to the square of the scattering angle. The scattering intensity in such a case is given by

$$S_1(q) = \frac{S_1(0)}{(1 + q^2\xi^2)^2} \tag{4}$$

In the present case, one expects to have one phase rich in PSD, but maybe containing a certain proportion of PUR,

Table 3. $S_1(0)$, the Correlation Length ξ_1, and the Specific Area S/V for Various Cross-Link Densities of PUR Networks Keeping the Density of PSD Fixed at 3% DVB

M_n(PUR)	% DVB	K^2_{max} (10^{-12} Å^{-4})	$S_1(0)$ (10^{-8} Å^{-1})	ξ_1 (Å)	specific area (10^2/m^2/g)	K^2 app (10^{-12} Å^{-4})	$A(10^{-4})$	B	q_{cross}
3025	3	34.4	6898.0	78.8	1.14	25.0	1.79	0.009	0.0127
2000	3	34.0	1189.0	44.7	2.00	23.6	2.99	0.007	0.0224
450	3	31.1	298.3	25.2	3.56	33.3			0.0397

Table 4. $S_1(0)$, the Correlation Length ξ_1, and the Specific Area S/V for Various Cross-Link Densities of PSD Networks with the Density of PUR Fixed at M_n = 2000

% DVB	M_n (PUR)	K^2_{max} (10^{-12} Å^{-4})	$S_1(0)$ (10^{-8} Å^{-1})	ξ_1 (Å)	specific area (10^2 m^2/g)	K^2_{app} (10^{-12} Å^{-4})	A (10^{-4})	B	q_{cross}
0	2000	35.8	1275.5	52.1	1.72	16.0	1.73	0.009	0.0192
3	2000	34.0	1189.0	44.7	2.00	23.6	2.99	0.007	0.0224
10.7	2000	29.5	995.1	39.8	2.26	28.0			0.0251

and a phase rich in PUR, but maybe containing a smaller fraction of PSD. Calling ϕ the volume fraction in the sample of the phase rich in PSD and translating from X-rays to neutron notations, $S_1(0) = 8\pi\xi_1{}^3K^2{}_{eff}\phi(1 - \phi)$, where $K^2{}_{eff}$ is the effective contrast between the two phases (cm^{-4} units). It can be expressed as a function, first, of $K^2{}_{max}$, the maximum contrast that would correspond to a complete separation of PSD in one phase and PUR in another and, second, of ϕ_1 and ϕ_2 which represent respectively, the volume fraction of the PSD in the phase rich in PSD and in the phase poor in PSD. Under this assumption, it is easy to show that

$$K^2{}_{eff} = K^2{}_{max}(\phi_1 - \phi_2)^2 \qquad (5)$$

Moreover conservation of species implies:

$$\phi\phi_1 + (1 - \phi)\phi_2 = \phi_{PSD} \qquad (6)$$

where ϕ_{PSD} represents the overall volume fraction of PSD in the sample.

Introducing $\delta\phi_1 = \phi_1 - \phi_{PSD}$, $\delta\phi_2 = \phi_2 - \phi_{PSD}$, one gets then

$$\phi(1 - \phi)(\phi_1 - \phi_2)^2 = -\delta\phi_1\delta\phi_2 \qquad (7)$$

Thus

$$K^2{}_{eff}\phi(1 - \phi) = K^2{}_{max}(\phi_1 - \phi_2)^2\phi(1 - \phi) = -K^2{}_{max}\delta\phi_1\delta\phi_2 \qquad (8)$$

From the limit for $\delta\phi_1$ ($0 < \delta\phi_1 < 1 - \phi_{PSD}$, $-\phi_{PSD} < \delta\phi_2 < 0$) one can show that always

$$K^2{}_{eff}\phi(1 - \phi) < K^2{}_{max}\phi_{PSD}(1 - \phi_{PSD}) \qquad (9)$$

In the case of perfect separation between PSD and PUR, one would get $\delta\phi_1 = 1 - \phi_{PSD}$ ($\phi_1 = 1$) and $\delta\phi_2 = -\phi_{PSD}$ ($\phi_2 = 0$). This gives back $K^2{}_{eff}\phi(1 - \phi) = K^2{}_{max}\phi_{PSD}(1 - \phi_{PSD})$.

In case of pure phases, $\phi = 0.34$ is the volume fraction for PUR and the other phase is PSD, and the contrast between the phases is estimated by us as $K^2{}_{max}$ at different cross-link densities as listed in Table 3 and 4 (where K_{max} is the contrast length density for neutron's and is defined as $(\psi_{PSD}\rho_{PSD} + \psi_{DVB}\rho_{DVB}) - (\psi_{POPG}\rho_{POPG} + \psi_{desN}\rho_{desN})$ where ρ_{PSD}, ρ_{POPG}, ρ_{DVB}, and ρ_{desN} are the scattering length densities and ψ_{PSD}, ψ_{POPG}, ψ_{DVB}, and ψ_{desN} are the volume fraction of PSD and DVB in the pure phase PSD/DVB, and POPG and Desmodur N in the pure PUR phase, respectively). However, there is no reason to assume that there will exist just two pure phases nor that there should exist just only two phases instead of multiple phases.

Table 5. $S_2(0)$ and the Correlation Length ξ_2 for Various Cross-Link Densities of PUR Networks with the Density of PSD Fixed at 3% DVB

sample	M_n (PUR)	% DVB	$S_2(0)$ (10^{-8} Å^{-1})	ξ_2 (Å)
W6	3025	3	10628.1	276.5
W3	2000	3	1341.8	213.5
W7	450	3	10476.4	687.0

Table 6. $S_2(0)$ and the Correlation Length ξ_2 for Various Cross-Link Densities of PSD Networks with the Density of PUR Fixed at a Precursor Mass M_n = 2000

sample	% DVB	M_n (PUR)	$S_2(0)$ (10^{-8} Å^{-1})	ξ_2 (Å)
W4	0	2000	1284.67	151.2
W3	3	2000	1341.8	213.5
W5	10.7	2000	4890.2	497.0

Fit of Data. Coming back to eq 4, we used the following procedure. First, in the regions 2 and 3, the square root of inverse intensity versus q^2 was fitted to a straight line. The y intercept $S_1(0)^{-1/2}$ yields the value of $S_1(q \rightarrow 0)$ while the x intercept gives the value $q^2{}_{cross} \approx 1/\xi_1{}^2$. We then fitted our data with the DB law (eq 4, $\xi = \xi_1$). It worked well in case of all samples at intermediate values of q. The characteristic lengths ξ_1 obtained for the samples varied from 20 to 80 Å as shown in Tables 3 and 4. In all cases we fitted the data using the largest possible value of ξ_1 to counteract effects of slight multiple scattering in the IPNs. It was not easy to fit the scattering from sample W7 to a Debye–Bueche because of a sharper fall of q^{-6} at large q.

The resulting Debye–Bueche (DB1) law yields a plateau at low q in contrast to our data at low q. The excess scattering in this range was taken care of by fitting the difference in scattering between the curve calculated by eq 4 and the data to another Debye–Bueche law (DB2), and we obtained $S_2(0)$ and ξ_2 (Tables 5 and 6). This gives another range of heterogeneities ξ_2 of the order of 150–700 Å. By using the same procedure initially used by Debye et al.[20] and then applied to SANS data for IPNs[8] by adding to Debye's original exponential correlation function (taking account of intermediate range interaction terms), another Gaussian term $\exp(-r^2/\xi_2)$ was developed which takes into account the long-range terms. In our case, using a second Debye-Bueche law worked better than fitting the data to an additional Gaussian term.

Large q Behavior. At high q, the asymptotic behavior of eq 4 is q^{-4}. For the less cross-linked samples, M_n = 3025 and 2000 (PUR) and 0% and 3% (PSD), a deviation, i.e. scattering greater than from the q^{-4} law, is observed. For these samples, plotting $q^4S(q)$ versus q^2 yields a straight line (for $q^2 > 0.05$), i.e. a $S(q) = (A/q^4) + (B/q^2)$ behavior (see Figure 4), where A is the intercept and B is the slope. A must agree with the DB1 law at large q

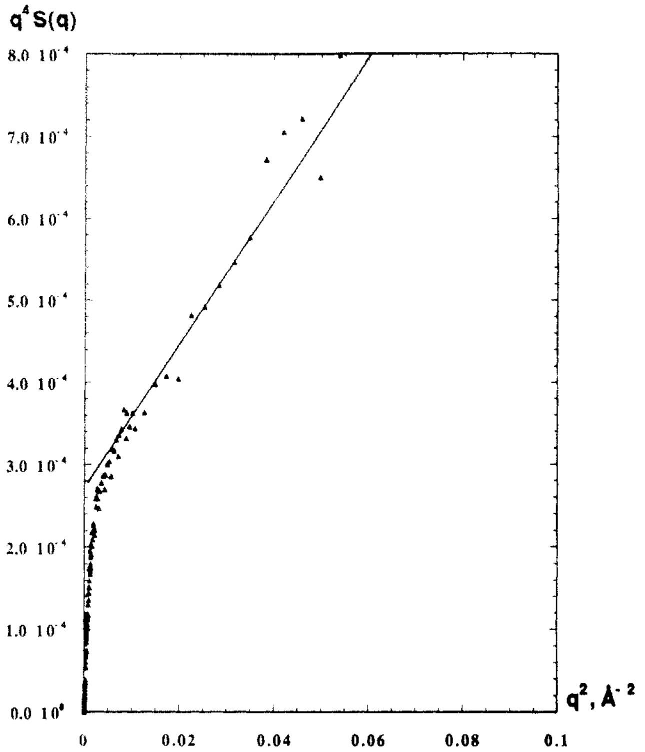

Figure 4. Plot of $q^4S(q)$ vs q^2 for M_n = 2000 and cross-link density of PSD fixed at 3% DVB.

$$S(q) \sim S'_1(q) = \frac{S_1(0)}{q^4\xi_1^{\,4}} = \frac{8\pi K^2\phi(1-\phi)}{\xi_1 q^4}$$

i.e.

$$A = \frac{8\pi K^2\phi(1-\phi)}{\xi_1}$$

In Porod's law, A is proportional to the specific surface, $A = 2\pi K^2 S/V$. Here, the specific area $S/V = [4\phi(1-\phi)/\xi_1]$ where S is the total surface area, V is the total volume. In Tables 3 and 4, A and S/V are given assuming maximum contrast; A and S/V increase with increasing cross-link density of PUR and PSD networks (while keeping the crosslink density of one of the networks of the IPN fixed). In principle, these values should be corrected by the actual value ϕ, ϕ_1, ϕ_2 which are unknown (see below). These measured values of S/V lies between 100 and 300 m^2/gm (assuming a density of 1 gm/cm^3), the latter being slightly larger than observed for poly(butadiene)/polystyrene[8] IPNs (160 m^2/gm), indicating a rather finely divided material.

By taking everything into account, the curves for W3, W4, and W6 are well approximated by

$$S(q) = \frac{S_1(0)}{(1+q^2\xi_1^{\,2})^2} + \frac{S_2(0)}{(1+q^2\xi_2^{\,2})^2} + \frac{B}{q^2} \qquad (10)$$

The last two terms being nominal correction terms at low and high q's respectively, the dominant scattering is accounted by the first Debye–Bueche (DB1) law. The results from such a fit are shown in Figures 5–7.

For the more strongly cross-linked samples W7 (M_n = 450, PUR) and W5 (10.7% DVB in PSD), a sharper falloff than q^{-4}, i.e. a q^{-6} law is observed at the large q values. No attempt was made to fit this behavior. It was checked that it cannot be modified qualitatively by changing the incoherent background subtraction within a large range, and we will discuss it below.

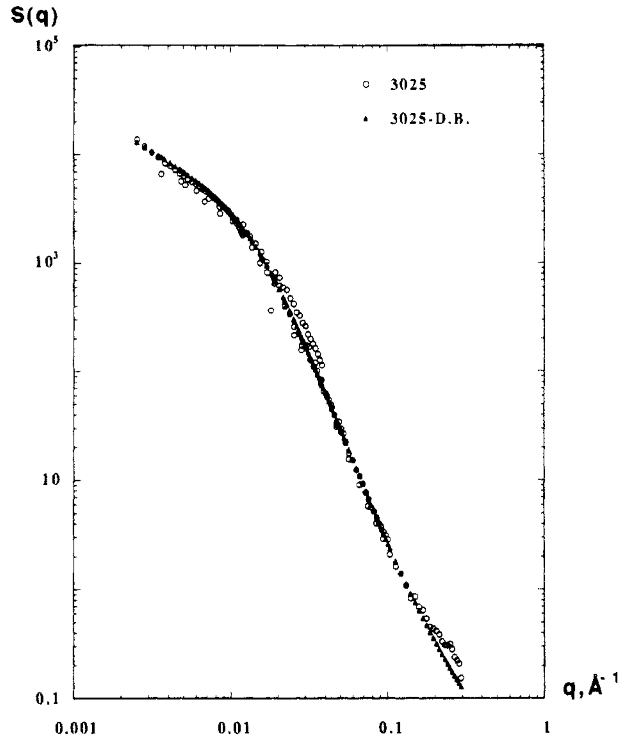

Figure 5. Plot of log $S(q)$ vs log q for PUR network with a precursor of mass M_n = 3025 and a PSD network with 3% DVB (open symbols) compared to fits of Debye–Bueche (full symbol) law using eq 10.

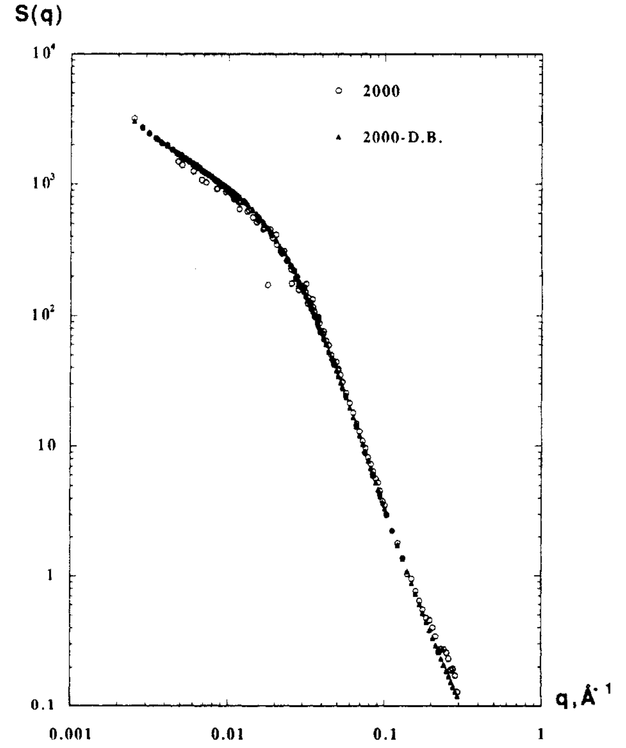

Figure 6. Plot of log $S(q)$ vs log q for PUR network with a precursor of mass M_n = 2000 and a PSD network with 3% DVB (open symbols) compared to fits of Debye–Bueche (full symbol) law using eq 10.

Effective Contrast and Phase Contents. Let us now discuss in more details the results given in Tables 3 and 4, considering first, $S_1(0)$ and ξ_1. The value of ξ_1 can be also directly obtained from the q axis. In principle, it is involved both in the value of $S_1(0)$ ($\approx\xi_1^{\,3}$) and of A ($\approx 1/\xi_1$), but is, in Å, convoluted with the factor $K^2_{\rm eff}\phi(1-\phi)$ (eq

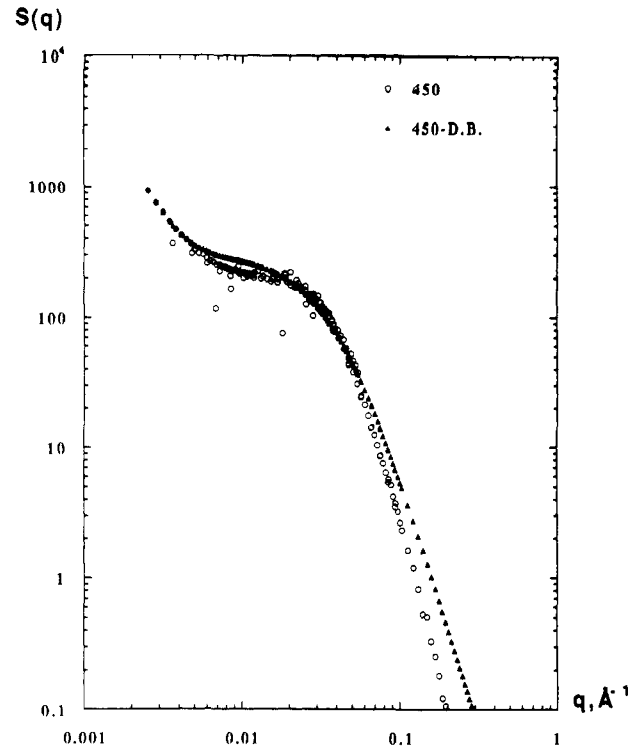

Figure 7. Plot of log $S(q)$ vs log q for PUR network with a precursor of mass M_n = 450 and a PSD network with 3% DVB (open symbols) compared to fits of Debye–Bueche (full symbol) law using eq 10.

9). We consider $K^2_{app} = [S_1(0)/8\pi\xi_1{}^3\phi_{PSD}(1-\phi_{PSD})]$ listed in Tables 3 and 4. If $K^2_{app} = K^2_{max}$, the phases are pure. K^2_{app} is increasing with increasing cross-linking.[22] For M_n = 450 (PUR) and 10.7% (PSD), K^2_{app} = 33.3 and 28.0 ($\times 10^{-12}$ Å^{-4}) is very close to the calculated value K^2_{max}. This could mean that for the most cross-linked samples the phases are almost pure. The segregation is to the greatest extent (even though the size of the regions is small). For the less cross-linked samples M_n = 3025, 2000 (PUR) and 0% and 3% (PSD), the factor is lower; each phase might be now more a mixture of PSD and PUR. Even though the size of the phase-separated domains is larger, the contrast is reduced. This is a direct consequence of $K^2_{app} < K^2_{max}$. However we do not know independently ϕ, ϕ_1, and ϕ_2, and thus we do not know $K^2_{eff} = [K^2_{app}\phi_{PSD}(1-\phi_{PSD})]/\phi(1-\phi)$, which can be higher or lower than K^2_{app} but always smaller than K^2_{max}). For instance, if $\phi_1 < 1$, but ϕ_2 remains zero, $\phi > \phi_{PSD}$, $\phi(1-\phi) < \phi_{PSD}(1-\phi_{PSD})$; and the opposite for $\phi_1 = 1$, $\phi_2 > 0$.

In the case of less segregated samples, the signal at large q can be coming from an incoherent addition of the scattering from the two phases:

$$S(q) \sim [\phi(1-\phi_1)\phi_1 + (1-\phi)(1-\phi_2)\phi_2]S_{1PSD}(q)K^2_{eff} \tag{11}$$

where $S_{1PSD}(q)$ is the single-chain form factor of PSD in PUR, which varies as $1/q^2$ at large q, as for any Gaussian chain in bulk. Such a signal may correspond to the B/q^2 term of eq 10.

Similar checks may be done on the value of A in relation with ξ_1 i.e.

$$\xi_1 A \approx 8\pi K^2_{eff}\phi(1-\phi) = \zeta \tag{12}$$

In other words, A and $S_1(0)$ are actually dependent on each other by a relation representing their crossover

$$S_1(q=1/\xi) = \frac{\zeta}{\xi_1 q^4} = \zeta\xi_1{}^3 = S_1(q=0) \tag{13}$$

Thus, the values of ξ_1 and $S_1(0)$ should determine the value of A or ζ. (K^2 is constant for a given sample.) This is however valid only within the Debye–Bueche model. The latter corresponds to a random distribution of objects. Here, the distribution could be different corresponding to either large or small sizes. The different values of ξ_1 correspond to $1/q_{cross}$, thus $S_1(0)$ and A or ζ will change with respect to each other. This would lead to an apparent contrast which might not be easy to determine.

Qualitative Explanation of Data: Microphase Separation. To separate completely the PUR network from the PSD, a finite number of the chemical bonds of the IPN will have to be broken or the chains of the network have to be extended, to result in domains which are richer in one component of considerable spatial extent. Hence, the extent of demixing is larger in less cross-linked state of the two networks of the IPN (this is evident from the values of ξ_1 and $S_1(0)$ in Tables 3 and 4).

In the case of weakly cross-linked networks Binder and Frisch[23] have derived wave vector dependent collective structure factor $S(q)$ due to local inhomogeneous changes in the volume fraction ϕ of species A (and $1-\phi$ of B) i.e. $\phi(\mathbf{r})$, around the value ϕ_0, which are slowly varying in space (ϕ_0 being the initial volume fraction of monomers of species A and thus $1-\phi_0$ for B)

$$S(q) = \left[\left(\frac{d^2f}{d\phi^2}\right)_{\phi_0} + \left(\frac{\sigma^2{}_A}{\phi_0} + \frac{\sigma^2{}_B}{1-\phi_0}\right)K(\phi_0)q^2\right]^{-1} \tag{14}$$

The $(d^2f/d\phi^2)\phi_0$ which enters here is the second derivative of the free energy density $f(\phi)$ for ϕ around ϕ_0. The second term is coming from the gradient square term, where the prefactors $\sigma^2{}_A$ ($\sigma^2{}_B$) are the monomer size of species A (B), $K(\phi_0)$ is the coefficient of the gradient energy term.

They consider the two interpenetrated networks (A and B) as independent, and thus add their elastic free energy in the form of $\phi F_{el\text{-}A}/k_BT + (1-\phi)F_{el\text{-}B}/k_BT$. They neglect a complicated topological connectivity term between the two networks and add an enthalpic interaction term of the Flory–Huggins type $\chi\phi(1-\phi)$. For the sequentially formed IPN, the volume fraction of preparation is 1 for network A, and $1-\phi_0$ for network B, the second derivative of free energy given by Binder and Frisch[23] is

$$\left(\frac{d^2f}{d\phi^2}\right)_{\phi_0} = -\frac{\phi_A{}^{2/3}(1)}{3N_A(1)}\phi_0{}^{-5/3} + \frac{B_A}{N_A(1)}\phi_0{}^{-1} - \frac{(1-\phi_B)^{2/3}(1-\phi_0)^{-5/3}}{3N_B} + \frac{B_B}{N_B}(1-\phi_0)^{-1} - 2\chi \tag{15}$$

The entropy of mixing of the two networks is assumed to be zero because of their infinite mass. The first term is the classical expression of the elastic energy of deformation of network A when being at concentration $\phi \approx \phi_0$ with respect to a fraction $\phi_A{}^*$ in the "reference state" (assumed to correspond to a state of no deformation), and the same for the third term for network B. [$(1-\phi_B{}^*)$ is the fraction of B in the reference state.] N_A and N_B is the effective number of monomer units between the two cross-links. The second term corresponds to the Wall–Flory logarithmic term.

The microphase separation that will take place will be due to the competition that will exist between the elasticity and the demixing terms. If both quantities $T_{el\text{-}A} = [-[(\phi_A/$

$\phi_0)^{2/3}/3] + B_A]$ (and the same with index B instead of index A) are negative, demixing will spontaneously occur for any value of χ and will be faster for larger $1/N_A$ and $1/N_B$ (i.e. for the most cross-linked systems). For larger $1/N_A$ ($1/N_B$), the peak in the scattering at the early stage will occur at larger $q \approx 1/N_A$. If T_{el} is positive, it may balance the -2χ term for high value of $1/N_A$ (i.e. for the large cross-linking ratio): cross-linking will delay phase separation.

The expression eq 14 combined with eq 15 can be compared with the thermodynamical derivation of the zero q limit scattering for a single network with solvent (gel)

$$S_{gel}(q=0) \approx \frac{k_B T}{(\kappa_{os\text{-}sol} - \mu/3 + B\mu)} \tag{16}$$

$\kappa_{os\text{-}sol}$ is the bulk osmotic modulus without cross-links (it is related to the non-zero entropy of mixing of the solvent and to χ); μ is the elastic modulus. Taking the expression 15 replacing the B term by a term including the entropy of solvent and taking $\mu \approx kT/N_A$

$$S_{gel}(q=0) \approx \frac{1}{(\kappa_{os\text{-}sol}/k_B T - {}^1/_3 N_A + B/N_A)} \tag{17}$$

which is similar to eq 16.

Taking $B = 0$, we obtain the expression $S_{gel}(q=0) \approx 1/(\kappa_{os\text{-}gel} - \mu/3)$ which increases with μ. Taking $B \approx 1$ or ${}^1/_2$, we obtain a decrease of the scattering with increasing cross-linking, similar to the expression often used $S_{gel}(q=0) \approx 1/(\kappa_{os\text{-}gel} - \mu/3 + 4\mu/3 + B\mu)$, where $4/3\mu$ represents the elastic energy of shear[24] and has been omitted in the reference.[23]

However, such expressions for $S(q)$ before demixing or during spinodal decomposition do not describe most of the experimental data, the observed q^{-4} dependence better corresponds to a well-advanced state of phase separation, although here also, the size of the demixed regions is limited by cross-linking: the origin is in a way similar to what was said just above, since cross-linking inhibits the formation of large clusters because their creation costs a lot of energy. An expression similar to single networks can be written for IPNs that would also predict a decrease of scattering on increased cross-linking.

For the most strongly cross-linked samples, $M_n = 450$ (PUR) and 10.7% (PSD), a falloff sharper than q^{-4} (Porod's law), i.e. a q^{-6} law is observed at the large q values. This law is usually seen for early stages of phase-separation kinetics. Furukawa[25] has predicted the asymptotic behavior of the scaled structure factor in phase-separating systems. The shape of the structure factor is determined by the coarsening mechanism in the phase-separating system. For $q > q_m$, i.e. the wave vectors greater than the characteristic length (q_m^{-1}) in the system, the asymptotic behavior of the structure factor varies as $S(q) = q^{-\gamma}$, where $\gamma = d + 1$ (Porod's scattering) when the phase-separated clusters are isolated and $\gamma = 2d$ when the clusters are not isolated but percolate through the structure and the interfaces of the clusters or droplets are entangled. Here, perhaps the same q^{-6} law is being observed at large values of q, for the strongly cross-linked samples, where we can expect a strong correlation between clusters.

Another alternative explanation is also proposed. At these large values of q, one could be sensitive to inter- or even intracorrelation of either monophasic objects or clusters of cross-links. For example, these correlations would lead to a minimum in $I(q)$ at $q \approx \pi/R$ where R is the radius of a spherically shaped object. There are oscillating terms in the scattering of finite-sized spherical particles. The maxima of scattering of such particles define an envelope $\approx q^{-4}$, with the first minima occurring at $q \approx \pi/R$. The intensity, as it drops toward the first minimum value, might do so with a slope greater than 4, i.e. 6. More generally, "correlation peaks" are predicted in regularly cross-linked systems[15] and appear in strongly cross-linked systems in the presence of trapped chains[13] or solvent[26,27,28] and for co-cross-linked PSD/PVME.[16] In the latter case, the subtraction of the signal given by the un-cross-linked mixture from the signal of the cross-linked one was proposed, which made clearly visible the maximum. Similarly, for sample W7 and W5 subtracting from data the DB law normalized with the highest q data would lead here to a defined maximum or shoulder, as observed in ref 10.

However there is a difference between our samples and those of ref 10. In the latter, a maximum in the scattering is found for a sample having one Tg, whereas sample displaying Porod's scattering have two Tg's. On the contrary, all the samples studied in this paper have two distinct Tg's. (Table 2).

IV. Summary and Conclusions

It is possible to describe the scattering as a superposition of several contributions:

In the intermediate q range, the signal is well described by a Debye–Bueche function characterized by a value $S_1(q \to 0)$ and a correlation length ξ_1 varying between 20 and 80 Å. Both decrease with increasing cross-link density. At large q, the Debye–Bueche law corresponds to a Porod's law A/q^4 where A is proportional to the specific area. The ratio $S_1(0)/\xi_1^3$ gives a value of the contrast which lies within the maximum value (in case of one pure PSD phase and one PUR phase) and half of it. This means that the difference between the two phases is strong. It is however noticeable that the contrast seems to be higher for the most cross-linked samples. This would mean that the two phases are more pure, unless it is due to a distortion of the size distribution, with respect to the random distribution implicitly contained in the Debye–Bueche law.

In the lower q range, another Debye–Bueche function is characterized by a value $S_2(q \to 0)$ and a correlation length ξ_2 represents heterogeneities larger than 200 Å. It is not known whether they correspond to microvoids of PSD often visible in a deuterated matrix (because vacuum–matrix contrast is higher) or to PSD–PUR heterogeneities of larger sizes. The largest signal corresponds to sample with $M_n = 3025$, for which there might even exist a phase separation between the POPG chains and the cross-links as the molecular weight of POPG chain is the highest. In this q regime, the pure PSD sample scatters much by itself, due to voids. It is not easy to decide what contribution to subtract from the signal of the IPNs, as one does not know the contribution of the voids. Consequently, for the most cross-linked sample, the low q signal could be due to voids, which on subtraction would lead to a maximum in $S(q)$.

In the large q regime, the less cross-linked samples tend to a q^{-2} law, which could be either due to a hairy interface or to the signal of the PSD–PUR mixture inside each phase (i.e. the signal of PSD chains in PUR-rich phase and PUR chains in the PSD-rich phase). On the contrary, the strongly cross-linked IPNs display a very steep decrease ($\approx q^{-6}$).

In comparison, a better developed peak is observed in the structure factor of simultaneously formed IPNs.[10] Maybe, in this case a microphase had time to develop into a periodic structure with a well-defined cutoff length, whereas here, in the case of in situ sequential IPNs, such a well-defined periodic structure is more difficult to form due the limiting presence of the first formed network.

In summary, it seems that most of the data, showing Debye–Bueche behavior, agree with the following picture: as the cross-link density is raised, the domains are smaller but purer in component content.

For the data exhibiting a "shoulder"—possibly related to a peak—it could have its origin due to the spinodal kinetics, but the q^{-4} law at large q makes us believe that relatively small demixed regions exist—it may be imagined that relatively dense segregated regions exist, but the correlation between these regions is reflecting the structure of highly cross-linked networks.

References and Notes

(1) Sperling, L. H. *Polym. Eng. Sci.* **1985**, *25*, 517.

(2) Tabka, M. T.; Widmaier, J. M.; Meyer, G. C. *Sound and Vibration Damping with Polymers*; Corsaro, R. D., Sperling, L. H., Eds.; ACS Symposium Series number 424, American Chemical Society: Washington, DC, 1992; Chapter 25, p 445.

(3) Nevissas, V.; Widmaier, J. M.; Meyer, G. C. *J. Appl. Polym. Sci.* **1988**, *36*, 1467.

(4) Lal, J.; Bastide, J.; Bansil, R.; Boué, F. *Macromolecules* **1993**, *26*, 6092.

(5) Jin, S. R.; Widmaier, J. M.; Meyer, G. C. *Polymer* **1988**, *29*, 346.

(6) McGarey, B., Richards, R. W. *Polymer* **1986**, *27*, 1315.

(7) McGarey, B.; Richards, R. W. *B. Polym. J.* **1987**, *19*, 111.

(8) An, J. H.; Fernandez, A. M.; Sperling, L. H. *Macromolecules* **1987**, *20*, 191.

(9) Fernandez, A. M.; Widmaier, J. M.; Sperling, L. H.; Wignall, G. D. *Polymer* **1984**, *25*, 1718.

(10) Brulet, A.; Daoud, M.; Zhou, P.; Frisch, H. L. *J. Phys. Fr.* **1993**, *3*, 1161.

(11) Donatelli, A. A.; Sperling, L. H.; Thomas, D. A. *J. Appl. Polym. Sci.* **1977**, *21*, 1189.

(12) Bansil, R.; Lal, J.; Carvalho, B. L. *Polymer* **1992**, *33*, 2961.

(13) Zielinski, F. H.; Buzier, M.; Lartigue, C.; Bastide, J.; Boué, F. *Prog. Colloid Polym. Sci.* **1992**, *90*, 115.

(14) Briber, R. M.; Bauer, B. J. *Macromolecules* **1991**, *24*, 1899.

(15) deGennes, P. G. *J. Phys. Lett.* **1979**, *40*, 69.

(16) Briber, R. M.; Bauer, B. J. *Macromolecules* **1988**, *21*, 3298.

(17) Boué, F. Thesis, University Paris Sud Orsay, 1982.

(18) Ragnetti, M.; Geiser, D.; Hocker, H.; Oberthur, R. C. *Makromol. Chem.* **1985**, *186*, 1701.

(19) Cotton, J. P. In *Neutron, X-ray, and Light Scattering*; Lindner, P., Zemb, T., Eds.; Elsevier: Amsterdam, 1991; Chapter 2, p 19.

(20) Debye, P.; Bueche, A. M. *J. Appl. Phys.* **1949**, *20*, 518.

(21) Debye, P.; Anderson, H. R., Jr.; Brumberger, J. *J. Appl. Phys.* **1957**, *28*, 679.

(22) Note: The variation, although systematic, is however not extremely strong and one must keep in mind that a relative error of 10% in ζ_1 could lead to a 30% error in this factor.

(23) Binder, K.; Frisch, H. L. *J. Chem. Phys.* **1984**, *81*, 2126.

(24) Onuki, A. In *Phase Transition in Polymer Gels*; Dusek, K., Ed.; Advances in Polymer Science; Springer: Berlin, manuscript in preparation.

(25) Furukawa, H. *Phys. Rev. B* **1986**, *33*, 638.

(26) Duplessix, R. Thesis, University Louis Pasteur, Strasbourg, France, 1975.

(27) Benoit, H.; Decker, D.; Duplessix, R.; Picot, C.; Rempp, P.; Cotton, J. P.; Farnoux, B.; Jannink, G.; Ober, R. *J. Polym. Sci. Polym. Phys. Ed.* **1976**, *14*, 2119.

(28) Mendes, E.; Lutz, P.; Bastide, J.; Boué, F. Manuscript in preparation.